Available online at www.sciencedirect.com

ScienceDirect

Procedia Structural Integrity 33 (2021) 528–543

Structural Integrity Procedia

www.elsevier.com/locate/procedia

IGF26 - 26th International Conference on Fracture and Structural Integrity

Considerations on the Thermoelastic Effect in proximity of crack tips on Titanium and Aluminium: a new formulation

Davide Palumbo[a], Rosa De Finis[a]*, Francesca Di Carolo[a], Umberto Galietti[a]

[a] *Department of Mechanics, Mathematics and Management, Politecnico di Bari, Via Orabona 4, 70125, Bari, Italy;*

Abstract

Thermoelastic Stress Analysis (TSA) is an experimental technique used for describing the stress state and the mechanical behaviour of materials subjected to linear-elastic deformations. The classic TSA theory consists of a simple relation between temperature and stress variations and was successfully applied in fracture mechanics for SIF and crack tip evaluation. This theory for some materials, such as titanium and aluminium, is no longer valid since the mechanical properties of the material cannot be neglected. The research framework lies in the field of the validity hypothesis of thermoelastic stress analysis, in this regard, the aim of this work is to present a new thermoelastic formulation that includes the second-order effects to investigate the thermoelastic effect in the proximity of crack tips, on Titanium and Aluminium. Moreover, error analysis has been carried out for investigating the differences between the proposed approach and the classical one.

Keywords: Thermoelastic Stress Analysis (TSA); Stress Intensity Factor (SIF); Titanium; Aluminium; mode I.

1. Introduction

The study and evaluation of the stress state in the proximity of the crack tip represents an important topic in many fields of engineering. In this regard, the Stress Intensity Factor (SIF) evaluation represents the main TSA application since the SIF together with the crack growth rate, provides important information on the fatigue behaviour of the material. SIF can be assessed by employing TSA (Thermoelastic Stress Analysis) Stanley, (1997), Lesniak et al (1997),Tomlinson et al (1997), Tomlinson et al (1999), Dulieu-Barton et al (2003),Diaz et al (2004),He and Rowlands

* Corresponding author. Tel.: +0-000-000-0000 ; fax: +0-000-000-0000 .
E-mail address: rosa.definis@poliba.it

10.1016/j.prostr.2021.10.059

(2004),Diaz et al (2005),Tomlinson (2011),De Finis et al (2016),Pitarresi et al (2019). This latter presents some advantages that make it suitable for on-line applications on real components under actual loading conditions. In particular, TSA requires an ease surface preparation unlike the other experimental techniques (an opaque paint is sufficient to ensure a high and uniform emissivity) and relatively simple set-up.

In the last years, many researchers adopted the TSA for obtaining the SIF value and assessing the crack tip. In his work, Stanley (1997) described the procedure for obtaining the Paris law parameters. The main advantage is that only a series of signal lines (horizontal or vertical) scanning around the crack-tip stress field and away from the plastic zone are required to obtain the SIF measurement. Pitarresi et al (2019) and Gupta et al (2015) provided estimations by taking into account the T-stress.

Dulieu-Barton et al. (2003) proposed a new curve-fitting routine based on a genetic algorithm for obtaining information about SIFs and crack tip in a mixed mode configuration. In this way, a more accurate evaluation of the crack tip was obtained.

All the cited works adopt the classical theory of TSA in which the changes of temperature are related to the changes of stresses through the thermoelastic constant for an isotropic material, in linear elastic conditions and under local adiabatic conditions according to Pitarresi and Patterson (2003).

In the works of Palumbo and Galietti (2010) and (2016) it was proposed a new procedure to process the thermoelastic data and to assess the correct value of the measured uniaxial stress. In particular, it was carried out an error analysis on titanium for investigating the mean stress effect on thermoelastic data and relative stress evaluation. This work demonstrated that significant errors in stresses evaluation can occur if the mean stress effect is neglected, above all in the presence of high-stress gradients.

More recently, Di Carolo et al. (2019) proposed a general TSA equation for studying the influence of biaxial residual stress on aluminium and titanium alloys. Through statistical analysis, the minimum value of residual stresses which leads to significant and measurable variations in TSA signal has been estimated. Moreover, it has been assessed the error in stress amplitude evaluation in the case residual stresses are neglected. This error depends on the modulus, direction and angle of the principal residual stresses with respect to the applied stresses.

Jones et al. (2006) in the appendix of their work, developed the thermoelastic equations considering the second order effects in the case of mode I fracture. They found that the thermoelastic temperature variation has also a harmonic component at the twice the loading frequency. Moreover, the thermoelastic signal presents the change of the order of singularity, from 0.5 to 1 due to the presence of the mean stress effect. However, they did not deeply investigate the effects on the SIF evaluation.

The aim of the present work is to present a new TSA formulation written in the proximity of crack tips that consider the variations of the material properties with temperature, in the presence of the mode I, on Titanium and Aluminium components. The proposed formulation accounts for the second-order effects (mean stress effect and the component at the twice of the mechanical frequency) that become significant for some materials like Titanium and Aluminium and can affect TSA applications in fracture mechanics, such as the SIF determination.

Starting from the revised TSA theory, the TSA equation has been developed by describing the stress state, in terms of principal stresses, at the crack tip using the Westergaard solution. Then, the new model was compared to the classic TSA equation through an error analysis for investigating the main parameters that could affecting the SIF measurement.

Nomenclature

a, b	Thermoelastic parameters
C_ε	Specific Heat at constant strain
E	Young' modulus
K_I	Stress Intensity Factor mode I
K_{II}	Stress Intensity Factor mode II
K_{min}	Minimum value of the Stress Intensity Factor
K_{max}	Maximum value of the Stress Intensity Factor
K_{Im}	Mean value of the Stress Intensity Factor
K_{Ia}	Amplitude value of the Stress Intensity Factor
P_{min}	Minimum value of the load
P_{max}	Maximum value of the load

$Q_{i,i}$	Heat flux through the surface of the body whose outward direct normal is n_i
r, θ	Polar coordinates
R	Stress ratio
s	First stress invariant
$\dot{s}$	First stress invariant rate
T	Reference temperature
$\dot{T}$	Temperature variation rate
α	Coefficient of linear thermal expansion
ε_{ij}	Strain tensor
$\dot{\varepsilon}_{ij}$	Strain tensor rate
$\dot{\varepsilon}_1$	Principal strain rate
$\varepsilon_{\Delta T}$	Absolute error in ΔT evaluation
$\varepsilon_{\Delta Tr\%}$	Percentage relative error in ΔT evaluation
ε_{KI}	Absolute error in K_I evaluation
$\varepsilon_{KI\,\%}$	Percentage relative error in K_I evaluation
ε_i	Principal strain
ε_{kk}	First strain invariant
δ_{ij}	Kronecker's delta
ΔT_{nc}	Non-correct value of temperature variations
ΔT_c	Correct value of temperature variations
μ, λ	Lamé constants
ρ_0	Density
σ_{ij}	Stress tensor
σ_i	Principal stress
$\dot{\sigma}_1$	Principal stress rate
σ_m	Mean uniaxial stress
σ_a	Amplitude uniaxial stress
υ	Poisson's ratio

2. Theory of Thermoelastic Stress Analysis

The thermoelastic effect, Stanley (1997) describes the change of temperature and the change of the sum of normal stresses for an isotropic material in linear elastic and adiabatic conditions. In particular, temperatures and stresses are related by the thermoelastic constant that is generally assumed to be constant independently on the applied stress.

For some materials, a linear dependence of the thermoelastic signal from the mean stress value is present (Belgen (1968)), the physical explanation of this effect and a review of the thermoelastic theory was presented by Wong et al. (1987). For an isotropic material without any internal heat source, the temperature variations can be described by the following equation:

$$\rho_0 C_\epsilon \dot{T} = T \frac{\partial \sigma_{ij}}{\partial T} \dot{\varepsilon}_{ij} - Q_{i,i} \tag{1}$$

where ρ_0 is the density of the material, C_ε is the specific heat under constant strain, T is the temperature, σ_{ij} is the stress tensor, ε_{ij} is the strain tensor (summing over i,j with $i,j=1\text{-}3$) and $Q_{i,i}$ is the heat flux through the surface of the body whose outward direct normal is n_i. The dotted symbols represent derivatives with respect to the time Wong et al. (1987). The constitutive law is:

$$\sigma_{ij} = 2\mu\varepsilon_{ij} + (\lambda\varepsilon_{kk} - \beta\Delta T)\delta_{ij} \tag{2}$$

with

$$\beta = (3\lambda + 2\mu)\alpha,\ \Delta T = T - T_0 \tag{3a}$$

$$\mu = \frac{E}{2(1+\nu)}, \qquad \lambda = \frac{\nu E}{(1+\nu)(1-2\nu)} \tag{3b}$$

where α is the coefficient of linear thermal expansion, λ and μ are the Lamé constants, T_0 is the reference temperature, ε_{kk} is the first strain invariant and δ_{ij} is the Kronecker delta.

By deriving the constitutive law with respect to the temperature and substituting into Eq. (1), yields the following relations, Wong et al. (1987):

$$T\left[\left(-\beta - \frac{\partial\beta}{\partial T}\Delta T + \frac{\partial\lambda}{\partial T}\varepsilon_{kk}\right)\delta_{ij} + 2\frac{\partial\mu}{\partial T}\varepsilon_{ij}\right]\dot{\varepsilon_{ij}} - \rho_0 C_\epsilon \dot{T} = Q_{i,i} \tag{4}$$

Under adiabatic conditions and expressing Eq. (4) in terms of principal strain ε_i :

$$\rho_0 C_\epsilon \frac{\dot{T}}{T} = -\left(\beta + \frac{\partial\beta}{\partial T}\Delta T - \frac{\partial\lambda}{\partial T}\varepsilon_{kk}\right)\dot{\varepsilon_{kk}} + 2\frac{\partial\mu}{\partial T}\varepsilon_i\dot{\varepsilon}_i \tag{5}$$

Substituting Eq. (3) in Eq. (5), neglecting the high order terms and the term $(\partial\beta/\partial T)\Delta T$ and expressing in terms of principal stresses [27], [28], we obtain:

$$\rho C_\varepsilon \frac{\dot{T}}{T} = -\left[\alpha + \left(\frac{\upsilon}{E^2}\frac{\partial E}{\partial T} - \frac{1}{E}\frac{\partial\upsilon}{\partial T}\right)s\right]\dot{s} + \left[\frac{(1+\upsilon)}{E^2}\frac{\partial E}{\partial T} - \frac{1}{E}\frac{\partial\upsilon}{\partial T}\right]\sigma_i\dot{\sigma}_i \tag{6}$$

where the symbol s represents the first stress invariant.

It is interesting to notice that for a one-dimensional stress state where the stress changes over time with a sinusoidal waveform, integrating Eq. (6), we obtain:

$$\rho C_\varepsilon \frac{\Delta T}{T_0} = -\left(\alpha - \frac{1}{E^2}\frac{\partial E}{\partial T}\sigma_m\right)\sigma_a \sin\omega t - \frac{1}{4E^2}\frac{\partial E}{\partial T}(\sigma_a)^2 \cos 2\omega t \tag{7}$$

where σ_m and σ_a represent the mean and the amplitude stresses respectively. Eq. (7) shows that the mean stress effect is strictly related to the Young modulus variation with the temperature. Moreover, it is interesting to observe that the thermoelastic signal occurs also at the twice of the loading frequency.

In the next section, the proposed approach will be presented by starting from Eq. (6) and considering a cracked material.

3. The proposed approach: a new formulation for describing the thermoelastic effect in proximity of crack tips

In this section, a new equation will be obtained for describing the thermoelastic behaviour of materials in the presence of a crack.

Two material constants can be defined as reported in Equation (8):

$$a = \frac{\alpha}{\rho C_\varepsilon},\ b = \frac{1}{E^2}\frac{\partial E}{\partial T}\frac{1}{\rho C_\varepsilon} \tag{8}$$

By considering the plane stress conditions, substituting Eq. (8) in Eq. (6) and neglecting the variations of the Poisson's ratio with the temperature, we obtain:

$$\frac{\dot{T}}{T} = -[a + \upsilon b(\sigma_1 + \sigma_2)](\sigma_1 \dot{+} \sigma_2) + (b + \upsilon b)(\sigma_1\dot{\sigma_1} + \sigma_2\dot{\sigma_2}) \tag{9}$$

Another important issue is represented by the plastic zone at the crack tip. It is well known that the stress values are limited by the yield stress of the material and then by the plastic behaviour that generates a stress redistribution around the crack tip. However, it is important to highlight that the aim of this work is to investigate the effect of second-order terms on the thermoelastic equation in the proximity of the crack. The effect of the plastic zone in TSA application has been extensively treated in literature by several authors in many works Lesniak et al (1997), Tomlinson et al (1997), Tomlinson et al (1999), Dulieu-Barton et al (2003), Diaz et al (2004), and, in this regard, methods and procedures based on the classical TSA equation (and its validity hypothesis), used for describing the stress state at the crack tip in the presence of the plastic area, can be extended in the same way to the new proposed formulation. In the present research it is not in the aim of the authors to make any speculation on plastic zone and its extension.

In presence of a crack in a flat plate, the state of the stress is characterized by two SIFs values, mode I and mode II, respectively, K_I and K_{II}. In this regard, Westergaard equations, Harwood and Cummings (1991), can be used for describing the state of stress around the crack in polar coordinates, as it is shown in Fig. 1 and Equation (10).

$$\begin{pmatrix}\sigma_x\\ \sigma_y\\ \tau_{xy}\end{pmatrix} = \frac{K_I}{\sqrt{2\pi r}}\cos\frac{\theta}{2}\begin{bmatrix}1-\sin\frac{\theta}{2}\sin\frac{3\theta}{2}\\ 1+\sin\frac{\theta}{2}\sin\frac{3\theta}{2}\\ \sin\frac{\theta}{2}\sin\frac{3\theta}{2}\end{bmatrix} + \frac{K_{II}}{\sqrt{2\pi r}}\begin{bmatrix}-\sin\frac{\theta}{2}\left(2+\cos\frac{\theta}{2}\cos\frac{3\theta}{2}\right)\\ \sin\frac{\theta}{2}\cos\frac{\theta}{2}\cos\frac{3\theta}{2}\\ \cos\frac{\theta}{2}\left(1-\sin\frac{\theta}{2}\sin\frac{3\theta}{2}\right)\end{bmatrix} \tag{10}$$

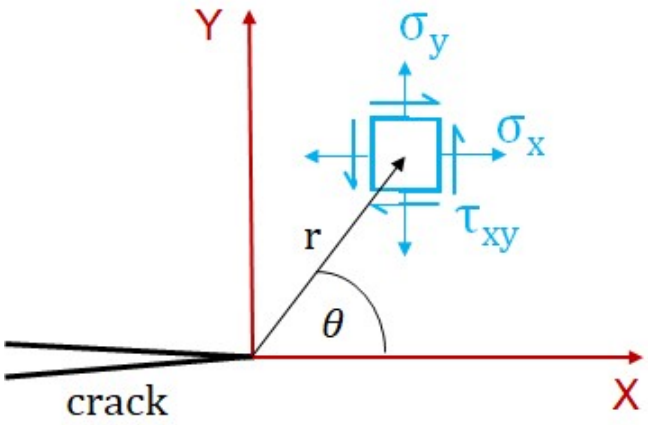

Fig. 1. Polar coordinates used for describing the stress state around the crack tip.

The principal stresses σ_1 and σ_2, can be obtained by applying Eq. (11):

$$\sigma_1, \sigma_2 = \frac{\sigma_x+\sigma_y}{2} \pm \sqrt{\left(\frac{\sigma_x-\sigma_y}{2}\right)^2 + \tau_{xy}^2} \tag{11}$$

Substituting Eq. (10) in Eq. (11) and considering only the mode I, the principal stresses are:

$$\sigma_1 = \frac{K_I}{\sqrt{2\pi r}}\cos\frac{\theta}{2}\left[1+sin\frac{\theta}{2}\right], \sigma_2 = \frac{K_I}{\sqrt{2\pi r}}\cos\frac{\theta}{2}\left[1-sin\frac{\theta}{2}\right] \quad (12)$$

Under a generic sinusoidal loading in which the load changes between its maximum and minimum values, P_{min} and P_{max}, the SIF ratio R can be defined as:

$$R = \frac{P_{min}}{P_{max}} = \frac{K_{Imin}}{K_{Imax}}, \qquad K_{Im} = K_{Ia}\frac{1+R}{1-R} = K_{Ia}R_f \quad (13)$$

with K_{Imin} and K_{Imax}, the minimum and maximum value of SIF and K_{Im}, K_{Ia} the mean and the amplitude values of SIF, respectively. In this way, the instantaneous value of SIF can be expressed as:

$$K_I(t) = K_{Im} + K_{Ia}\sin\omega t = K_{Ia}(R_f + \sin\omega t) \quad (14)$$

and the principal stresses and their rate of change, become:

$$\sigma_1 = \frac{K_{Ia}}{\sqrt{2\pi r}}\cos\frac{\theta}{2}\left[1+sin\frac{\theta}{2}\right](R_f+\sin\omega t),\ \sigma_2 = \frac{K_{Ia}}{\sqrt{2\pi r}}\cos\frac{\theta}{2}\left[1-sin\frac{\theta}{2}\right](R_f+\sin\omega t) \quad (15)$$

$$\dot{\sigma_1} = \frac{K_{Ia}}{\sqrt{2\pi r}}\cos\frac{\theta}{2}\left[1+sin\frac{\theta}{2}\right]\omega\cos\omega t,\ \ \dot{\sigma_2} = \frac{K_{Ia}}{\sqrt{2\pi r}}\cos\frac{\theta}{2}\left[1-sin\frac{\theta}{2}\right]\omega\cos\omega t \quad (16)$$

In the same way, the first stress invariant and its rate can be obtained:

$$\sigma_1+\sigma_2 = \frac{2K_{Ia}}{\sqrt{2\pi r}}\cos\frac{\theta}{2}(R_f+\sin\omega t), \qquad (\sigma_1 \dot{+} \sigma_2) = \frac{2K_{Ia}}{\sqrt{2\pi r}}\cos\frac{\theta}{2}\omega\cos\omega t \quad (17)$$

Substituting Equations (15), (16) and (17) in Eq. (9), neglecting the static components, we obtain an equation that can be expressed as the sum of two functions f_1 and f_2 multiplied for $cos(\omega t)$ and $sin(2\omega t)$:

$$\frac{\dot{T}}{T} = f_1\cos\omega t + f_2\sin 2\omega t \quad (18)$$

Where

$$f_1 = -\left[\frac{a\omega}{\sqrt{2\pi r}} + \frac{vb\omega}{\pi r}K_{Ia}\cos\frac{\theta}{2}R_f\right]2\cos\frac{\theta}{2}K_{Ia} + b(1+v)\left[\frac{\omega}{\pi r}K_{Ia}^2\cos^2\frac{\theta}{2}R_f\left(1+\sin^2\frac{\theta}{2}\right)\right] \quad (19)$$

and

$$f_2 = \frac{vb\omega}{\pi r}\cos^2\frac{\theta}{2}K_{Ia}^2 + b(1+v)\left[\frac{\omega}{2\pi r}K_{Ia}^2\cos^2\frac{\theta}{2}\left(1+\sin^2\frac{\theta}{2}\right)\right] \quad (20)$$

By integrating Eq. (18), considering $\Delta T << T_0$, we have finally the general expression of the thermoelastic signal (temperature variation) in the proximity of the crack:

$$\frac{\Delta T}{T_0} = g_1\sin\omega t + g_2\cos 2\omega t \quad (21)$$

where

$$g_1 = -\left[\frac{a}{\sqrt{2\pi r}} + \frac{\upsilon b}{\pi r} K_{Ia} \cos\frac{\theta}{2} R_f\right] 2\cos\frac{\theta}{2} K_{Ia} + b(1+\upsilon)\left[\frac{1}{\pi r} K_{Ia}^2 \cos^2\frac{\theta}{2} R_f \left(1+\sin^2\frac{\theta}{2}\right)\right] \quad (22)$$

And

$$g_2 = \frac{\upsilon b}{2\pi r}\cos^2\frac{\theta}{2} K_{Ia}^2 - b(1+\upsilon)\left[\frac{1}{4\pi r} K_{Ia}^2 \cos^2\frac{\theta}{2}\left(1+\sin^2\frac{\theta}{2}\right)\right] \quad (23)$$

Equations (22) and (23) show as the thermoelastic signal presents also terms in which the order of singularity is 1 induced by the presence of second-order effects, as already noted by Jones et al. (2006).

Putting $b=0$ in Eq. (21) leads the classical solution used for relating the thermoelastic signal and K_{Ia}:

$$\Delta T_{nc} = -T_0 \frac{2aK_{Ia}}{\sqrt{2\pi r}} \cos\frac{\theta}{2} \sin\omega t \quad (24)$$

where ΔT_{nc} stands for the non-correct value of ΔT.

Comparing Equations (21) and (24), it is worth to notice that the thermoelastic temperature variation ΔT depends also on the stress ratio R and on the material constants b and υ. This means that an error in ΔT evaluation and then in SIF evaluation can be made in using Equation (24) instead of Eq. (21).

In the next section, the results obtained with the new equation will be shown for titanium and aluminium and a comparison with the classical approach will be performed.

4. Results and discussion

Equations (21) and (24) can be used for obtaining analytically the map of ΔT if the mechanical and thermo-physical constants of material are known.

In the proposed equation (Eq. 21) the thermoelastic temperature variation now consists of two harmonic components at ω and 2ω. The thermographic data are processed via hardware or software, Harwood and Cummings (1991), to extract, separately, the amplitude and phase images related to the first and second harmonic of the thermoelastic signal. In this regard, the temperature variation, ΔT_c, obtained by the new formulation can be represented as:

$$\Delta T_c = (g_1 T_0)\sin\omega t + (g_2 T_0)\cos 2\omega t = \Delta T_{c1}\sin\omega t + \Delta T_{c2}\cos 2\omega t \quad (25)$$

4.1 Procedure for obtaining synthetic TSA data using the proposed formulation

TSA data can be obtained from Equation (25). In this way, we can obtain the thermoelastic effect induced temperature variations at ω and 2ω as:

$$\Delta T_{c1}(r,\theta) = T_0\left\{-\left[\frac{a}{\sqrt{2\pi r}} + \frac{\upsilon b}{\pi r} K_{Ia}\cos\frac{\theta}{2} R_f\right] 2\cos\frac{\theta}{2} K_{Ia} + b(1+\upsilon)\left[\frac{1}{\pi r} K_{Ia}^2 \cos^2\frac{\theta}{2} R_f\left(1+\sin^2\frac{\theta}{2}\right)\right]\right\} \quad (26)$$

$$\Delta T_{c2}(r,\theta) = T_0\left\{\frac{\upsilon b}{2\pi r}\cos^2\frac{\theta}{2} K_{Ia}^2 - b(1+\upsilon)\left[\frac{1}{4\pi r} K_{Ia}^2 \cos^2\frac{\theta}{2}\left(1+\sin^2\frac{\theta}{2}\right)\right]\right\} \quad (27)$$

Equations (26) and (27) can be rewritten as a function of K_{Imax} and the stress ratio R. In this case, we can write:

$$K_{Ia} = K_{Imax}\left(\frac{1-R}{2}\right) \tag{28}$$

and then, substituting in Equations (26) and (27):

$$\Delta T_{c1}(r,\theta) = T_0\left\{-\left[\frac{a}{\sqrt{2\pi r}} + \frac{\upsilon b}{2\pi r}K_{Imax}\cos\frac{\theta}{2}(1-R)\right]\cos\frac{\theta}{2}K_{Imax}(1-R) + b(1+\upsilon)\left[\frac{1}{4\pi r}K_{Imax}^2\cos^2\frac{\theta}{2}(1-R^2)\left(1+\sin^2\frac{\theta}{2}\right)\right]\right\} \tag{29}$$

$$\Delta T_{c2}(r,\theta) = T_0\left\{\frac{\upsilon b}{8\pi r}\cos^2\frac{\theta}{2}K_{Imax}^2(1-R)^2 - b(1+\upsilon)\left[\frac{1}{16\pi r}K_{Imax}^2(1-R)^2\cos^2\frac{\theta}{2}\left(1+\sin^2\frac{\theta}{2}\right)\right]\right\} \tag{30}$$

Equations (29) and (30) can be used for obtaining the thermoelastic temperature variation as a function of the polar coordinates r and θ if the material constants (a, b, υ) and the experimental test parameters (R, K_{Imax}) are known. In particular, the procedure for obtaining the synthetic ΔT_c maps consists in:

1. Setting the input parameters: the material constants (a, b, υ) and test parameters (R, K_{Imax}).
2. Defining a region of interest (ROI) in rectangular coordinates (X,Y) where x_{max} and y_{max} represent the maximum values of the coordinates expressed as *mm* unit.
3. Discretizing the ROI considering a geometrical resolution in terms of millimetre/pixel (*mp*). n_x and n_y represent the number of pixels along X and Y, respectively.
4. Assessing the polar coordinates for each pixel $r(x,y)$ and $\theta(x,y)$.
5. Assessing ΔT_{c1} and ΔT_{c2} for each pixel by using Equations (29) and (30).

The procedure to obtain the synthetic thermoelastic data (ΔT_c maps) is also shown graphically in Fig. 2. In Table 1 are reported the mechanical and thermo-physical properties used for generating the synthetic data for the titanium alloy Ti6Al4V. In Table 1 are also reported the properties of the aluminium alloy AA6082, Di Carolo et al (2019), that will be investigated in next subsections. As an example, in Fig. 3 are shown the results for the titanium alloy Ti6Al4V considering $R=0.1$, $K_{Imax}=70\ MPa(m)^{1/2}$ and a resolution of *0.05 mm/pixel* for a ROI of 20x20 mm^2. It is worth to notice that the chosen value of K_{Imax} is very close to the fracture toughness of the material and leads to emphasize the difference between the two TSA formulations (classical vs. proposed) for the imposed value of R.

In Fig. 3, the TSA maps a) and c) refer to the new and classic formulations respectively, while the map b) refers to the temperature variations occurring at the twice of the loading frequency (2ω). Comparing the new equation, ΔT_{c1}, with the classical one, ΔT_{nc}, it can be seen how the presence of second-order effects produces a different temperature distribution around the crack tip. In the next section, a quantitative comparison between the two TSA equations will be shown and possible consequences in SIF evaluation will be investigated.

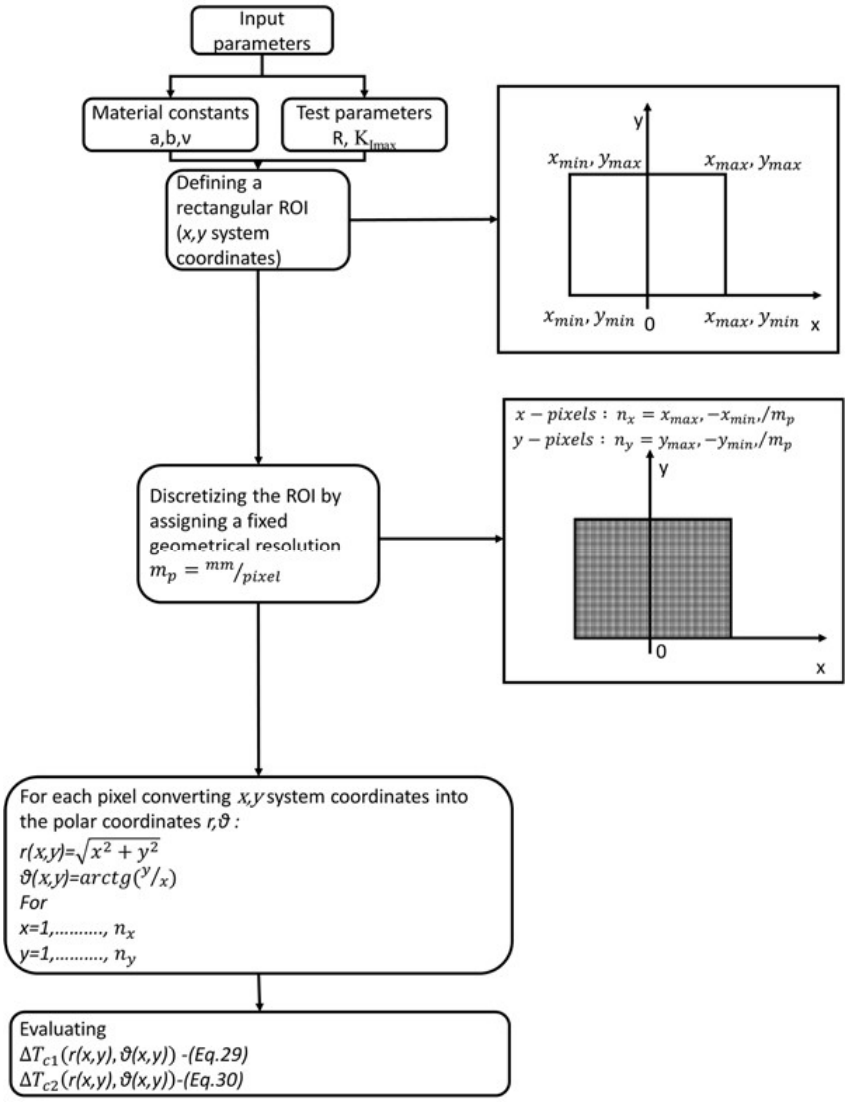

Fig. 2. Procedure used for obtaining the thermoelastic maps ΔT_{c1} and ΔT_{c2}.

Table 1. Mechanical and thermo-physical properties of the considered materials. [1] The specific heat at constant strain was obtained by considering $C_p = C_\varepsilon$.

Material	**α (K^{-1})**	**ρ (Kg/m^3)**	**C_p (J/KgK)**	**C_ε [1] (J/Kg·K)**	***E* (GPa)**	**υ**	***∂E/∂T* (MPa/K)**	**$R_{p0.2}$ (MPa)**	***b/a* (MPa^{-1})**
AA6082	23.2×10^{-6}	2.70×10^3	890	890	70	0.33	−36	260	3.17E-04
Ti6Al4V	8.6×10^{-6}	4.43×10^3	560	560	114	0.34	−48	1100	4.31E-04

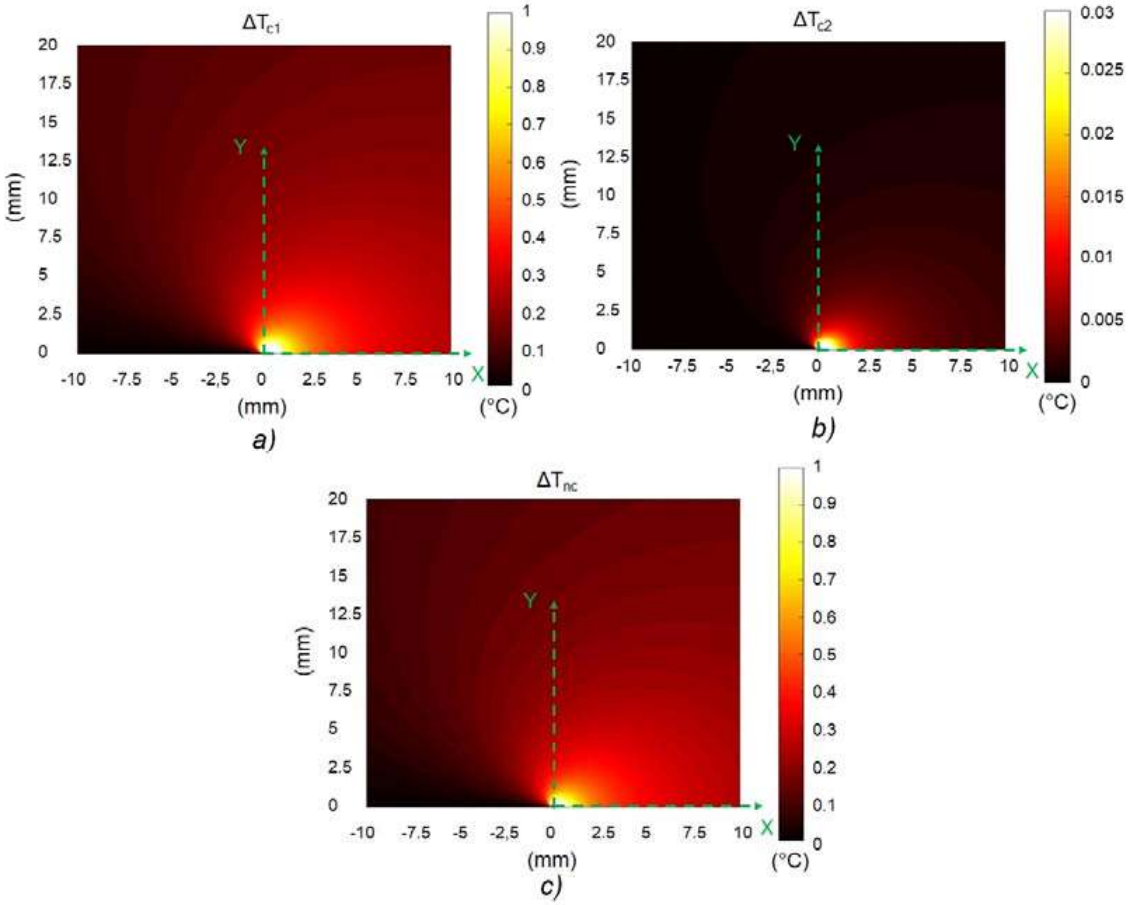

Fig. 3. Thermoelastic maps obtained by using synthetic data ($R=0.1$, $K_{Imax}=70\ MPa(m)^{1/2}$, resolution of *0.05 mm/pixel* for a ROI of *20x20 mm²*): a) Thermoelastic map representing the induced temperature variations at ω, Eq. 26, b) Thermoelastic map representing the induced temperature variations at 2ω, Eq. 27, c) Thermoelastic map representing the induced temperature variations at ω, Eq. 24.

4.2 Experimental implications in TSA applications

In previous sections, a new formulation has been assessed for describing the thermoelastic temperature variations in the presence of cracks. To study quantitatively the effect of second-order terms on TSA equations, an analytical expression will be used for estimating the error committed with the classical approach in the ΔT evaluation. In this regard, the absolute error expression for ΔT ($\varepsilon_{\Delta T}$), can be assessed by considering only the first harmonic term (angular frequency ω):

$$\frac{(\Delta T_{nc}+\varepsilon_{\Delta T})}{T_0}=\frac{\Delta T_{c1}}{T_0}=g_1 \Rightarrow \varepsilon_{\Delta T}=\Delta T_{c1}-\Delta T_{nc} \tag{31}$$

Substituting Equations (24) and (26) in Equation (31), we obtain:

$$\varepsilon_{\Delta T}=T_0\left\{\frac{b}{\pi r}{K_{Ia}}^2\cos^2\frac{\theta}{2}R_f\left[1-\upsilon+\sin^2\frac{\theta}{2}+\upsilon\sin^2\frac{\theta}{2}\right]\right\} \tag{32}$$

and rewriting Eq. (32) as a function of K_{Imax}:

$$\varepsilon_{\Delta T}=T_0\left\{\frac{b}{4\pi r}{K_{Imax}}^2\cos^2\frac{\theta}{2}(1-R^2)\left[1-\upsilon+\sin^2\frac{\theta}{2}+\upsilon\sin^2\frac{\theta}{2}\right]\right\} \tag{33}$$

Equation (33) shows the absolute error in ΔT evaluation $\varepsilon_{\Delta T}$, depends on:

- the material properties b and υ,
- the polar coordinates r and θ,
- the square of K_{Imax} and the SIF ratio R.

To have a comparison between different materials, the use of the relative error can be used:

$$\varepsilon_{\Delta Tr\%} = \left|\frac{\varepsilon_{\Delta T}}{\Delta T_{c1}}\right| * 100 \tag{34}$$

It is important to highlight that Equations (33) and (34) provide theoretical errors and represent only an analytical tool for estimating the difference between the proposed formulation and the classical one. A complete error analysis should involve the study of the error sources and the uncertainty evaluation. This analysis will be the object of further works.

In Fig. 5 and 6, are reported results in terms of thermoelastic temperature variations ΔT and the relative error $\varepsilon_{\Delta Tr\%}$ for three different cases, for the titanium and the aluminium alloy. In Table 1, are reported the material constants, while in Tables 2 and 3 are shown the values of variables R, θ, r and K_{Imax} used for each case. It is important to underline that the values in Tables 2 and 3 were only used to study the behaviour of the new equation (Eq. 29) and to show how this latter differs with respect to the classical TSA equation (Eq. 24). As already said in Introduction, the effect of the plastic conditions has been consciously neglected since the present work is focused on the presenting a new formulation for TSA equations.

Fig. 5 and 6, a) and b), show the effect of the polar coordinate r, Fig. c) and d) show the effect of the SIF ratio R and Fig. e) and f) show the effect of the polar coordinate θ on the relative error. In the same way, the effect of θ and R has been investigated by adopting a step of $1°$ and 0.1, respectively.

In each case, the error can become significant if values of ΔT are considered in the proximity of the crack tip and with a positive SIF ratio away from -1. In particular, it is interesting to notice that the maximum relative error presents its maximum values around $\theta=90°$ with fixed values of r and R.

Table 2. Values of the parameters used for investigating the relative error (Ti6Al4V).

Case	***r (mm)***	***θ (°)***	***R***	***K_{Imax} Ti6Al4V (MPa(m)$^{1/2}$)***
1	*(2÷10) step=0.1*	60	0.1	70
2	2	60	*(-1÷0.9) step 0.1*	70
3	2	*(0÷180) step 1*	0.1	70

Table 3. Values of the parameters used for investigating the relative error (AA6082).

Case	***r (mm)***	***θ (°)***	***R***	***K_{Imax} AA6082 (MPa(m)$^{1/2}$)***
1	*(2÷10) step=0.1*	60	0.1	30
2	2	60	*(-1÷0.9) step 0.1*	30
3	2	*(0÷180) step 1*	0.1	30

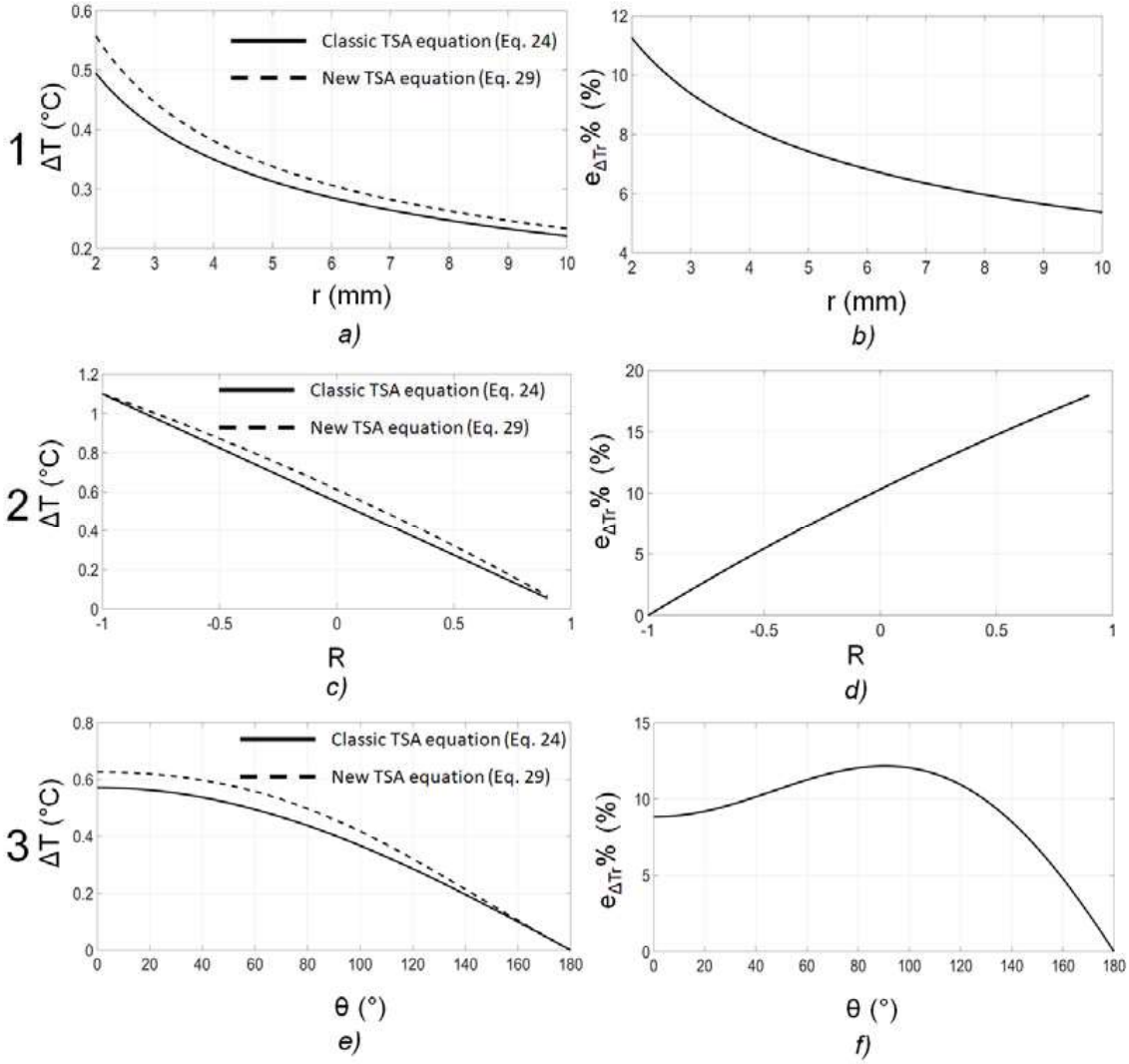

Fig. 5. Thermoelastic temperature trends ΔT and relative errors for the titanium alloy Ti6Al4V: a), c) and e) thermoelastic temperature trend as a function of r, R and θ, b), d), f) relative error trend as a function of r, R and θ.

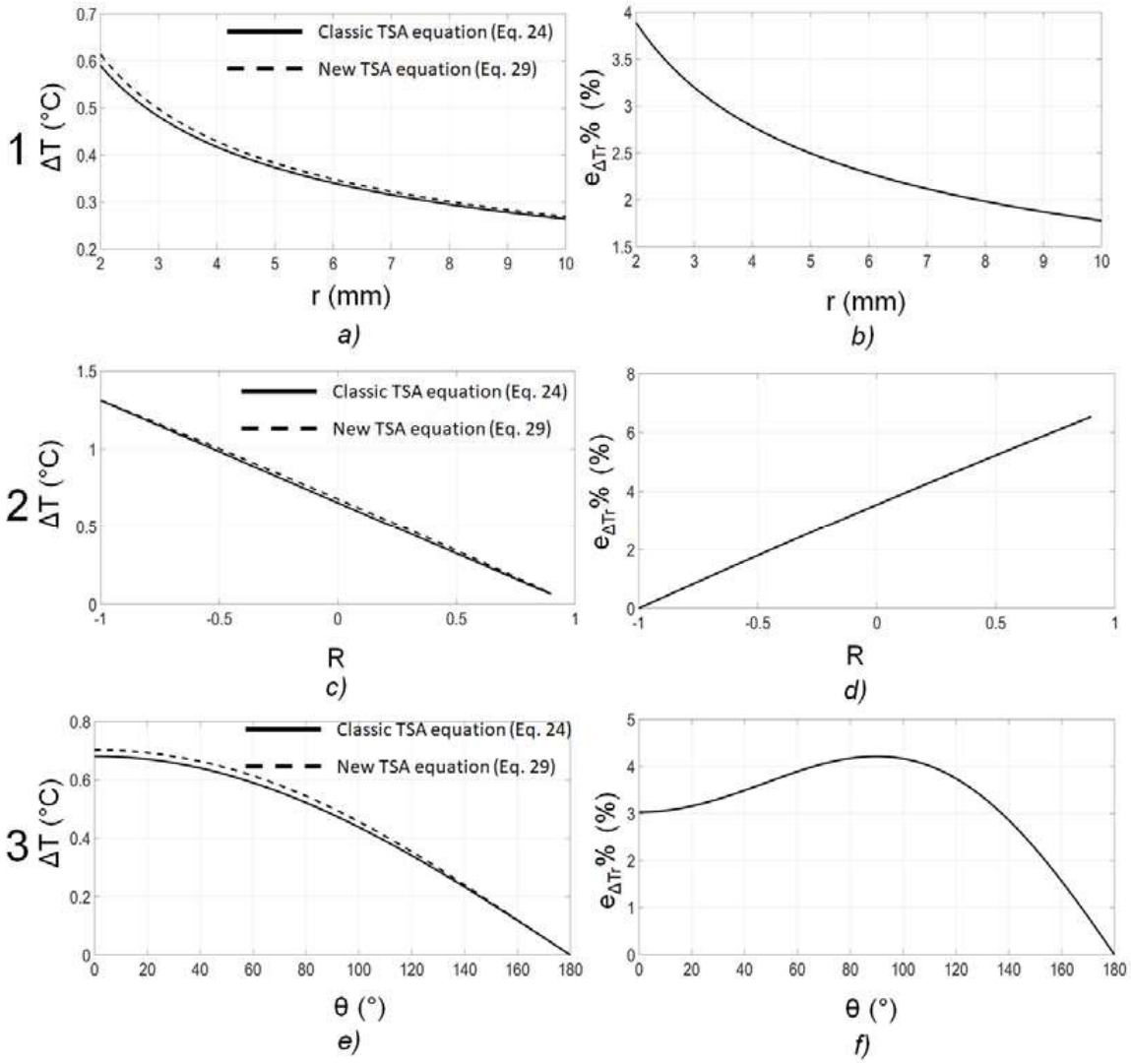

Fig. 6. Thermoelastic temperature trends ΔT and relative errors for the aluminium alloy AA6082: a), c) and e) thermoelastic temperature trend as a function of r, R and θ, b), d), f) relative error trend as a function of r, R and θ.

4.3 Experimental implications in SIF evaluation

The new TSA formulation appears different from the classical one. In particular, the SIF and temperature variations are no longer directly related by only the constant of material a. In this regard, the main implication in SIF evaluation with experimental data is that the Stanley method Stanley (1997), is no longer valid. All the TSA approaches described in Introduction for SIF evaluation can be applied by considering Eq. (29) and by knowing the material constants b and υ. However, these approaches can be still applied, but a significant error can be committed depending on the material and adopted test parameters.

In this case, the absolute error in SIF evaluation can be obtained by considering the following relation:

$$\frac{\Delta T_{c1}}{T_0} = -\frac{2a}{\sqrt{2\pi r}}\cos\frac{\theta}{2}(K_{Ia} + \varepsilon_{KI}) = g_1 \tag{35}$$

Substituting Equation (22) in (36), we obtain:

$$\varepsilon_{KI} = \frac{b}{a}\frac{1}{\sqrt{2\pi r}}{K_{Ia}}^2\cos\frac{\theta}{2}R_f\left[\upsilon - \upsilon\sin^2\frac{\theta}{2} - \sin^2\frac{\theta}{2} - 1\right] \tag{36}$$

and expressing all in terms of SIF ratio R and K_{Imax}:

$$\varepsilon_{KI} = \frac{1}{4}\frac{b}{a}\frac{1}{\sqrt{2\pi r}} {K_{Imax}}^2 \cos\frac{\theta}{2}(1-R^2)\left[\upsilon - \upsilon\sin^2\frac{\theta}{2} - \sin^2\frac{\theta}{2} - 1\right] \tag{37}$$

The relative error can be obtained:

$$\varepsilon_{KIr\%} = \left|\frac{\varepsilon_{KI}}{K_{Ia}}\right| * 100 \tag{38}$$

$$\varepsilon_{KIr\%} = \left|\frac{1}{2}\frac{b}{a}\frac{1}{\sqrt{2\pi r}} K_{Imax}\cos\frac{\theta}{2}(1+R)\left[\upsilon - \upsilon\sin^2\frac{\theta}{2} - \sin^2\frac{\theta}{2} - 1\right]\right| * 100 \tag{39}$$

Equation (40) shows that the relative error depends on:

- the material properties b/a and υ,
- the polar coordinates r and θ,
- K_{Imax} and the SIF ratio R.

Also, in this case, Equations (37) and (39) represent the theoretical error if the second order effects (mean stress) are neglected and describe how the new formulation differs from the classical one. In this way, Equations (37) and (39) are useful, for the specific material to estimate the error made by using the classic TSA theory under specific test conditions. In this regard, it is important to highlight that the experimental SIF evaluation cannot be obtained by a single point analysis and depends on the method used for TSA data processing.

In Fig. 7, the graphs related to the error trends are reported for each material (Tables 1) and each case of Table 2. The maximum errors occur for $\theta \approx 90°$ and linearly depends on the SIF ratio R.

It is worth noting that, the error is higher for titanium than aluminium and that the titanium alloy Ti6Al4V presents a higher ratio b/a than aluminium (Table 1). This result was expected since the ratio b/a represents the sensitivity of the thermoelastic parameter to the mean stress variations.

The results of Fig. 7 show that the error of second order effects can be significant in SIF evaluation above all for titanium that presents higher mechanical properties than aluminium.

5. Conclusions

In this work, a new formulation has been proposed for describing the TSA signal in proximity of a crack tip on titanium and aluminium. The proposed approach starts from the revised theory of the TSA in which it is considered the effect of the mean stress on the thermoelastic signal.

The thermoelastic equation has been rewritten for describing the stress distribution around a crack by using Westergaard equations. The main results can be summarized as follows:

- A part of the thermoelastic equation occurs at twice of loading frequency. This component depends on the square of the SIF and it is independent from the stress ratio.
- The component of the thermoelastic signal that occurs at the load frequency depends on the material properties and the stress ratio.

The possible effects in the SIF evaluation has been investigated in the case when the classical thermoelastic equation is used. In this case, the main results show that the relative error depends on:

- The material properties b/a and υ,
- the values of the polar coordinates r and θ,
- K_{Imax} and the SIF ratio R.

Finally, it has been shown that the second order effects are significant above all for titanium since it presents a high sensitivity to the mean stress and higher mechanical properties than aluminium.

The proposed equation of the theoretical error can be a useful tool to understand the limits of applicability of classical theory and then when the new formulation is demanded. Further works will be focused on possible experimental

approaches to obtain the SIF with the proposed formulation.

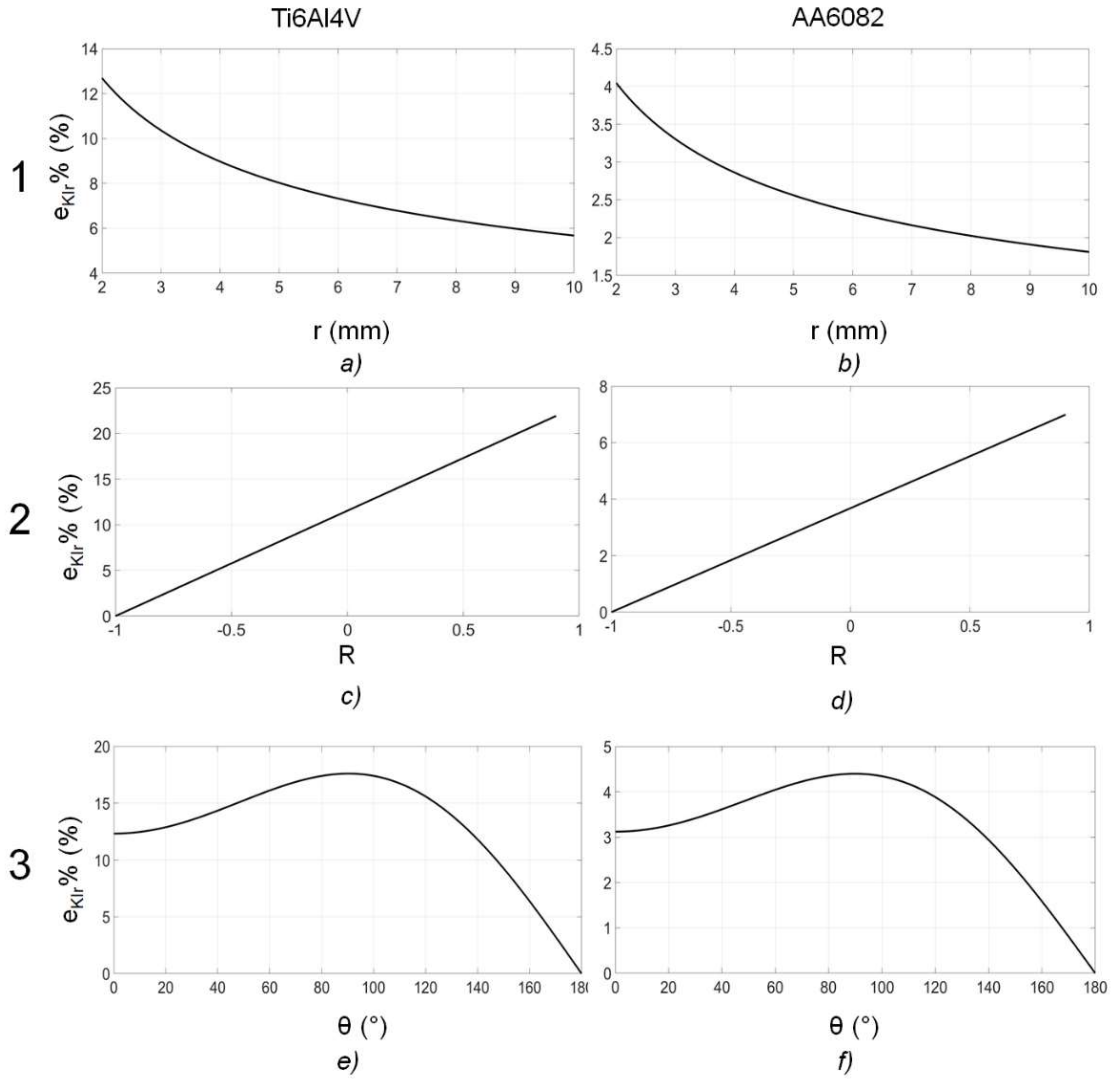

Fig. 7. Relative error trends in SIF evaluation for both materials: a), c) and e) error trend as a function of r, R and θ, for the titanium alloy Ti6Al4V b), d), f) error trend as a function of r, R and θ, for the aluminium alloy AA6082.

References

Stanley, P., 1997. Applications and potential of thermoelastic stress analysis. J Mater Process Tech 64, 359-370.

Lesniak, J., Bazile, D., Boyce, B., Zichel, M., Cramer, K. , Weich, C.,1997. Stress Intensity Measurement via Intensity Focal Plane Array, in Nontraditional Methods of Sensing Stress, Strain, and Damage in materials and Structures, ed. G. Lucas and D. Stubbs (West Conshohocken, PA: ASTM International, 208-220.

Tomlinson, R.A. , Nurse, A.D. , Patterson, E.A., 1997. On determining stress intensity factors for mixed mode cracks from thermoelastic data. Fatigue Fract Engng Mater Struct 20(2), 217-226.

Tomlinson, R.A. , Olden, E.J. , 1999. Thermoelasticity for the analysis of crack tip stress fields – review. Strain 35, 49-55.

Dulieu-Barton, J.M., Worden, K., 2003. Genetic identification of crack-tip parameters using thermoelastic isopachics. Meas Sci Technol 14,176-183.

Diaz, F.A.; Patterson, E.A.; Tomlinson, R.A.; Yates, J.R. Measuring stress intensity factors during fatigue crack growth using thermoelasticity. Fatigue Fract Eng Mater Struct 2004 26(4), 571-583.

K.Y. He, R.E. Rowlands, Determining stress intensity factors in orthotropic composites from far-field measured temperatures. Exp Mech 44 (2004) 555-561.

F.A. Diaz, E.A. Patterson, J.R. Yates, Differential Thermography Reveals Crack Tip Behaviour ?, in Proceedings 2005 SEM Annual Conference on Experimental Applied Mechanics, Society for Experimental Mechanics, 2005, Portland, OR, USA, 6–9 June 2005, pp. 1413–1419.

R.A. Tomlinson, E.A. Patterson, Examination of Crack Tip Plasticity Using Thermoelastic Stress analysis, Thermomechanics and Infra-Red

Imaging, in: Proceedings of the Society for Experimental Mechanics Series 2011, Volume 7, Springer, New York, NY.

R. De Finis, D. Palumbo, U. Galietti, Mechanical behaviour of stainless steels under dynamic loading: An investigation with thermal methods, J. Imaging 2(4) (2016), 32.

G. Pitarresi, M. Ricotta, G. Meneghetti, Investigation of the crack tip stress field in a stainless steel SENT specimen by means of thermoelastic stress analysis. Procedia Struct Integr 18 (2019) 330-346.

M. Gupta, R.C. Alderliesten, R. Benedictus, A review of T-stress and its effects in fracture mechanics, Eng Fract Mech 134 (2015), 218-241.

N. Harwood, Cummings, W.M. Thermoelastic Stress Analysis; Adam Hilger: Philadelphia, PA, USA, 1991.

G. Pitarresi, E.A Patterson, A review of the general theory of thermoelastic stress analysis, J. Strain Anal. Eng. Des. 38(2003), 405–417.

A.L. Gyekenyesi, G.Y. Baaklini, Thermoelastic Stress Analysis: The Mean Stress Effect in Metallic Alloys, in Proceeding of SPIE 3585, Nondestructive Evaluation of Aging Materials and Composites III, Newport Beach, CA, USA, 8 February 1999.

A.L. Gyekenyesi, G.Y. Baaklini, Quantifying Residual Stresses by Means of Thermoelastic Stress Analysis, in Proceeding of SPIE 3993, Nondestructive Evaluation of Aging Materials and Composites IV, Newport Beach, CA, USA, 13 May 2000.

Wong, R. Jones, J.G. Sparrow, Thermoelastic constant or thermoelastic parameter?, J. Phys. Chem. Solids 48 (1987), 749–753.

F. Di Carolo, R. De Finis, D. Palumbo, U. Galietti, A Thermoelastic Stress Analysis General Model: Study of the influence of Biaxial Residual Stress on Aluminium and Titanium, Metals 9(6) (2019), 671.

F. Di Carolo, R. De Finis, D. Palumbo, U. Galietti, Study of the thermo-elastic stress analysis (TSA) sensitivity in the evaluation of residual stress in non-ferrous metal, in Thermosense: Thermal Infrared Applications XLI 2019; Baltimore; United States; 15 April 2019 through 17 April 2019; Code 151454, Volume 11004, Article number 110040O.

U. Galietti, D. Palumbo, Thermoelastic Stress Analysis of Titanium Components and Simultaneous Assessment of Residual Stress, in Proceeding of EPJ Web of Conferences, ICEM 14—14th International Conference on Experimental Mechanics, Poitiers, France, 4–9 July 2010; p. 38012.

D. Palumbo, U. Galietti, Data correction for thermoelastic stress analysis on titanium components, Exp. Mech. 56 (2016), 451–462.

R. Jones, S. Pitt, An experimental evaluation of crack face energy dissipation. Int J Fatigue 28 (2006) 1716-1724. doi:10.1016/j.ijfatigue.2006.01.009.

M.H. Belgen, Infrared Radiometric Stress Instrumentation application range study, NASA contractor report, NASA CR-1067, 1968.

N. Harwood, Cummings, W.M. Thermoelastic Stress Analysis; Adam Hilger: Philadelphia, PA, USA, 1991.